Nanofiber optic sensor based on the excitation of surface plasmon wave near fiber tip

Yu-Jen Chang
Yi-Chun Chen
Hui-Ling Kuo
Pei-Kuen Wei
Academia Sinica
Research Center for Applied Sciences
128, section 2, Academia Road, Nankang
Taipei 11529, Taiwan
E-mail: pkwei@gate.sinica.edu.tw

Abstract. We present a sensitive nano-optical fiber biosensor made by shaping a fiber to form a taper with a tip size under 100 nm. A 40-nm-thick layer of gold is coated around the tapered fiber and a surface plasmon wave is excited near the tip to achieve a sensitivity of the reflective index unit of ~4000 (% RIU^{-1}) in the intensity measurement. A 3-D coded finite-difference time-domain approach verifies the excitation of the surface plasmon wave and the differences among its intensities in media of various refractive indices. The nanotip fiber sensor has the merits of a low background light and an ultrasmall detection region. Only a microliter of sample solution is required for detection.
[DOI: 10.1117/1.2165171]

Keywords: fiber optical sensor; surface plasmon wave; nanostructure.

Paper 05103R received Apr. 21, 2005; revised manuscript received Aug. 10, 2005; accepted for publication Sep. 30, 2005; published online Jan. 24, 2006.

1 Introduction

Optical excitations of surface plasmon waves (SPWs) on metallic surfaces are applied extensively for biosensing.[1] The conventional approach employs attenuated total reflection (ATR) to excite an SPW on a gold film at the bottom of a prism. ATR biosensors are known to be very sensitive to changes in the surface environment. They resolve the refractive index unit (RIU) to the order of 10^{-6} in a precise angular measurement.[2] The ATR setup is typically bulky and expensive and requires a large amount of sample solution. The other popular way to excite SPWs is based[3–5] on directional coupling between waveguide modes and SPWs. Among waveguide-coupling devices, fiber-based SPW sensors have attracted much attention because they are light, can be used in remote sensing, and have multiplexing potential. A typical fiber-based SPW sensor narrows the diameter of a fiber to several micrometers by using flame torch or polishing method. Metals such as gold or silver are coated on the tapered waist region. Guiding optical waves in a fiber are coupled to SPWs when they satisfy the phase-matching condition. Some of the waveguide modes are coupled to SPW mode, reducing the intensity of transmitted light. Measuring optical intensity changes gives information about the environmental medium. However, the fiber sensor must be several millimeters long to couple light to SPWs efficiently. Microfluidic channels are usually required to fill the sensing area with the sample solution.

Recently, Mitsui et al.[6] proposed a probe-type fiber optic sensor by coating nanoparticles onto the end of the fiber. Localized surface plasmon resonance (LSR) was excited by the evanescent waves generated by the scattering of light by the nanoparticles. The coupling of evanescent waves to the LSR depends on the changes to the surface environment.[7,8] The highest RIU resolution was $\sim 10^{-5}$ with this method. However, most incident light does not interact with the nanoparticles. Less light was coupled to SPWs than was coupled by previous fiber optical SPW sensors. This causes a large background to the LSR signals. This paper presents another probe-type fiber optic sensor that uses a nanometer fiber tip. Coating metal around the fiber tip confines the optical wave near the tip to a region that is smaller than its wavelength. Large evanescent waves are present near the tip.[9] They can be coupled to SPWs when the phase-matching condition is met. The SPWs can propagate on the surface of the gold film and radiate from the end of the tip. Nevertheless, the optical waves not coupled to SPWs are confined to the tip and cannot propagate to the far field because of their evanescent characteristics. Therefore, the SPW dominates the measured far-field intensity at the tip, yielding a sensitive and low-background signal. In the experiments herein, a refractive index resolution of up to 2×10^{-5} RIUs at a power stability of 0.1% can be achieved using only microliter sample solution.

2 Theoretical Model and Simulations

The basic idea that underlies generating SPWs in the fiber tip is phase matching at the tapered tip. Figure 1(a) depicts the excitation of SPWs at the tapered fiber tip that is coated with a thin gold film. The guiding wave in the core of the fiber interacts with the gold film in the tapered tip region. The incident light is at an angle (θ) to the normal of the gold film. The SPW is generated at the gold surface, if the incident angle satisfies the phase-matching condition,

Address all correspondence to Pei-Kuen Wei, Academia Sinica, Research Center for Applied Sciences, 128, section 2, Academia Road, Nankang, Taipei 11529, Taiwan. Tel.: 886–2–27898000; Fax: 886–27826680; E-mail: pkwei@gate.sinica.edu.tw

1083-3668/2006/11(1)/014032/5/$22.00 © 2006 SPIE

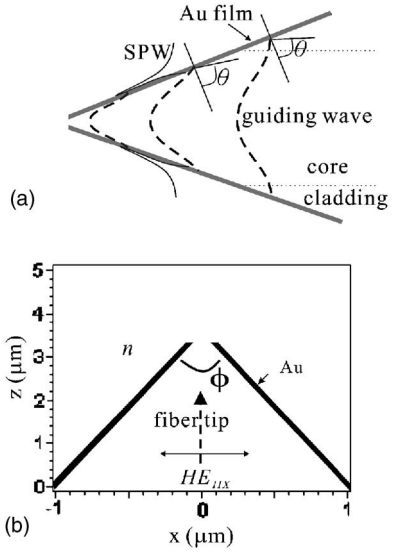

Fig. 1 (a) SPW excitation at the tapered fiber tip. The fiber tip is coated with a thin gold film. The SPW is generated at the gold surface, if the incident angle satisfies the phase-matching condition. Notably, the incident angle is not a constant. (b) The calculation domain in the 3-D finite-difference time-domain simulation of light in a nanotip. The fiber cone has a refractive index of 1.5. The fiber cone is coated with a 40-nm-thick gold layer; the dielectric constant of gold is −12.5. The fiber cone has a tapered angle of 30 deg. Outside the gold coating is the medium. The perfect matching layer conditions apply at all boundaries.

$$n \sin \theta = \left(\frac{\varepsilon_c \varepsilon_m}{\varepsilon_c + \varepsilon_m} \right)^{1/2}, \tag{1}$$

where n denotes the refractive index of glass, and ε_m and ε_c are the dielectric constants of gold and the surrounding medium, respectively. The incident angle is $\pi/2 - \phi/2$, where ϕ is the tapering angle of the fiber. At $n=1.5$, $\varepsilon_m=1.33$, and a tapered angle of 30 deg, the SPW is generated at $\varepsilon_m=-11.24$. This value is close to the dielectric constant of gold at a wavelength of 650 nm, revealing that SPW is generated in the tip region and propagates to the end of the tip when a red laser (650 nm) is coupled to the tapered fiber tip. The SPW coupling efficiency depends on the phase-matching condition. The output light intensity can be used to measure the refractive index of the surrounding medium. Notably, the incident angle θ is not fixed near the tip region. The 3-D tapered cone of the fiber probe focuses light on a tiny spot. The light travels toward the tip of the probe. The incident angle at the metal/glass interface is gradually increased, as shown in Fig. 1(a). Therefore, phase matching for a higher refractive index medium occurs closer to the tip, where the optical intensity in the probe is much stronger. The coupling of SPWs is expected to increase with the refractive index of the surrounding medium.

A 3-D finite-difference time-domain (FDTD) method[10] was used to simulate the propagation of light in a nanotip and thus confirm the generation of SPWs at the gold-coated fiber tip and the effect of environmental changes on the SPW signals. The FDTD simulations directly differentiate the Maxwell equations in both the temporal and the spatial domains. No assumptions were required in calculating the propagation of light. This fact is important because lateral wave vectors are large when light propagates in a structure whose feature size is well below its wavelength. The extensively employed beam propagation method, based on the paraxial assumption, does not apply in this case. Figure 1(b) presents the calculation domain in the XZ plane. The parameters in the calculation were as follows; the length of each grid cell was 20 nm in each of the x, y, and z directions. The fiber cone had a tapering angle of 30 deg and a tip diameter of 80 nm. The glass fiber had a refractive index of 1.5. Outside the fiber cone was a thin gold-coated layer. The dielectric constant of gold was −12.5. Outside the gold coating was the surrounding medium. The refractive index of the medium was 1.33 to simulate the fiber tip in water. The boundaries were all defined according to the perfect matching layer (PML) conditions. Reflected light from boundaries was negligible because the PML conditions applied at all boundaries.

A light source was launched from the fiber core and the optical intensity at the tip region was calculated. The incident light was a HE11 mode, as determined in a 2-μm fiber core. The wavelength of the light was 650 nm. The incident light was linearly polarized. Its polarization direction was parallel to the x axis. The circular symmetry of the tapered probe was such that other linear polarizations, such as y polarization, yielded the same result. Figures 2(a) and 2(b) present the electric field distributions in both the XZ and the XY planes. The XZ image clearly shows the presence of SPWs at the gold/medium interface near the tip region. The SPW is generated at the tapered region and can propagate to the tip. Figure 2(b) plots the XY plane electric field distribution at the end of the tip. The figure displays two lobes in the x direction. The lobes are SPWs that propagate from the tapered region to the tip end. The tapered tip and the metallic coating confine most light in the probe to a tiny spot (~80 nm), and the radiation of SPW at the end of the tip is important in the transmission efficiency. In the simulation, the transmission efficiency is $\sim 1.8 \times 10^{-2}$. Comparing optical intensities at the tip's opening and the lobes in Fig. 2(b), the SPW contributes over 50% of the intensities of the transmitted light.

The thickness of the gold film is known to affect the coupling efficiency of SPW. The transmission intensity was calculated for gold films of various thicknesses of gold to determine the best thickness value. The refractive index of the surrounding medium varied from 1.33 to 1.4. Figure 2(c) plots the calculated results. We used $I(n)/I(n=1.33)$ was used to normalize the transmission intensity to the referenced medium (water). The figure provides some important information concerning the nanofiber SPW sensor. First, it confirms that the transmission of light increases with the refractive index of the surrounding medium. Second, the optimal gold film thickness is around 50 to 60 nm. A thinner gold film corresponds to smaller changes in intensity because the SPW is weaker and more light is transmitted in the tip. Increasing the thickness of the gold film increases the coupling of SPW. However, when thickness of the gold layer exceeds 80 nm, the coupling of SPW is reduced. At the case of $\phi=30$ deg, $\lambda=650$ nm, and a film thickness of 50 nm, the transmission intensity can be increased by a factor of 1.4 when the outside refractive index is changed from 1.33 to 1.4. Third, the transmission intensity increases linearly with the refractive index of the surrounding

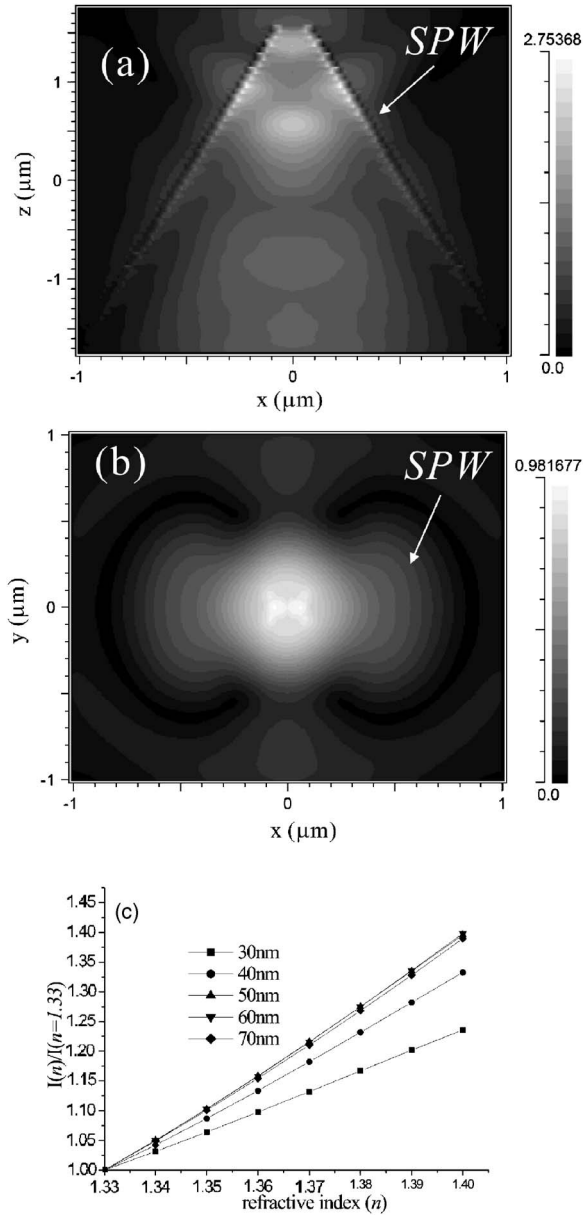

Fig. 2 (a) Calculated electric field in the *XZ* plane. The incident wavelength was 650 nm and was *x*-polarized. The SPW is generated in the tapered region and propagates to the tip end. (b) Electric field at the end of the tip, viewed in the *XY* plane. The field is not circularly symmetric. Two lobes are formed by the generation of the SPWs at the gold/medium interface. (c) Optical intensities for various thicknesses of the gold film with various external media. The ~50-nm Au film was the most sensitive. The intensity increases by a factor of ~1.4 as the outside refractive index changed from 1.33 to 1.4.

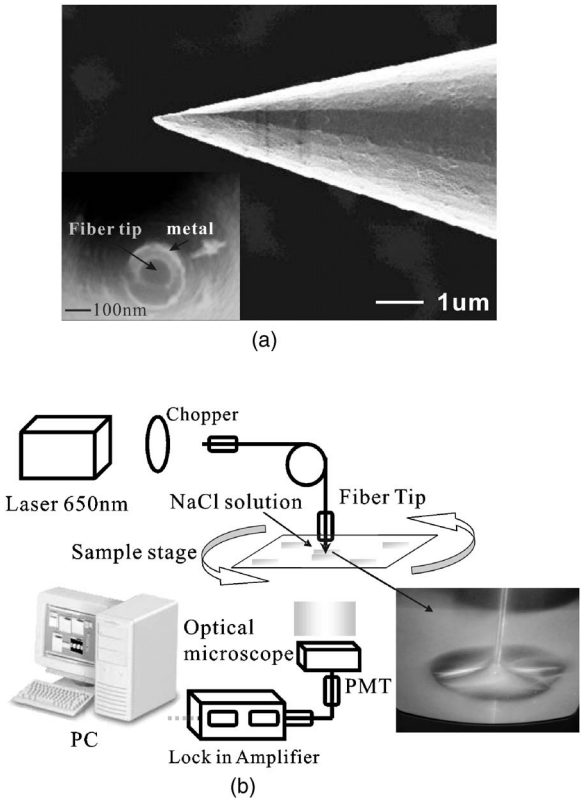

Fig. 3 (a) SEM image of fiber tip region. The fiber was made from a 635-nm single-mode optical fiber, etched using 45% HF solution. The inset displays the results of gold coating. (b) Setup of the SPW measurement system. A 650-nm-wavelength solid-state laser was coupled to the fiber. The laser was modulated using an optical chopper. NaCl solutions of various concentrations were dropped onto a glass slide. The transmission light was collected using a 10× objective lens and detected using a photomultiplier tube (PMT). A lock-in amplifier read the modulated optical signals and sent the intensity value to a computer.

medium. The correlation coefficient R between the data and the linear fit exceeds 0.99. Notably, the fittings at larger slopes have larger deviations; for instance, $R=0.993$ for the 50-nm film while $R=0.9998$ for the 25-nm film.

3 Experimental Setup and Results

The key component of the fiber probe sensor is the tapered fiber tip with a smooth surface. The tip was prepared using a modified wet-etching method, described elsewhere.[11] Figure 3(a) presents a scanning electron microscope (SEM) image of the fiber tip region. The fiber was made from a 635-nm single-mode optical fiber (3M FS-SN3224), etched using 45%HF solution. A smooth surface and a shaped tip were obtained after an etching time of 60 min. The fiber was then coated with a 40-nm-thick layer of gold around the tip region. The inset in Fig. 3(a) presents the results of coating with gold. The gold-coated fiber tip was placed in a microscopic system to measure the refractive index of the solutions. Figure 3(b) depicts the setup of the measurement system. A linearly polarized laser with a wavelength of 650 nm was modulated using an optical chopper at a frequency of ~1 kHz. It was coupled to the fiber from the cleaved end and generated a tiny optical spot at the tapered tip. NaCl solutions of various concentrations were dropped on a glass slide using a micropipette. The volume of each drop was 2 μl. The concentrations of NaCl were 0, 3.5, 5, 7.5, 10, 14.5, and 20% mg/cm^3 After it had interacted with a NaCl solution, the transmission light was collected by a 10× objective lens and detected using a photomultiplier tube (PMT). A lock-in amplifier read the modulated optical signals and sent the intensity values to a computer. Figure 4(a) plots the measured intensity versus the

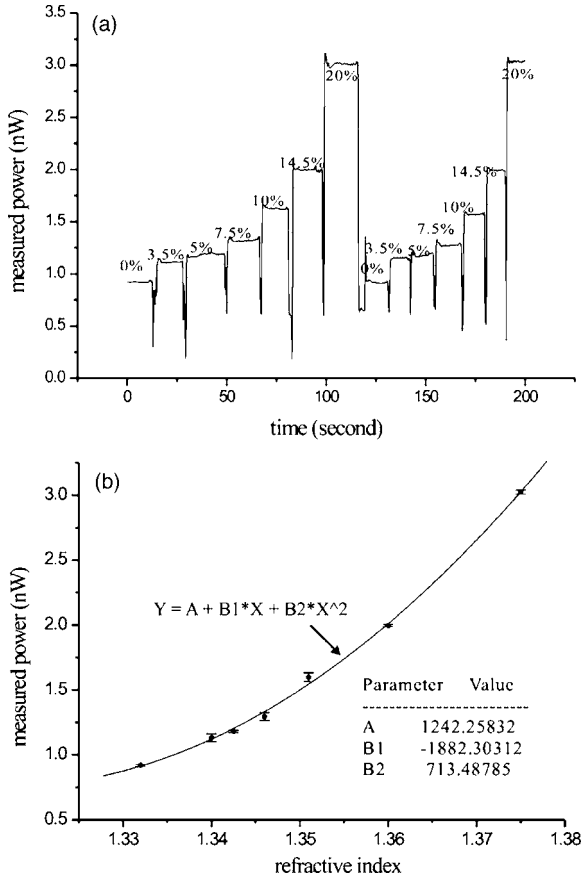

Fig. 4 (a) Optical intensity versus salt concentration. The concentrations of NaCl were 0, 3.5, 5, 7.5, 10, 14.5, and 20% mg/cm^3. The figure shows two repeated circles. (b) Optical intensity versus refractive index. The plot confirms that the transmission intensity increased with the surrounding refractive index. The RIU sensitivity is ~4444 (% RIU^{-1}).

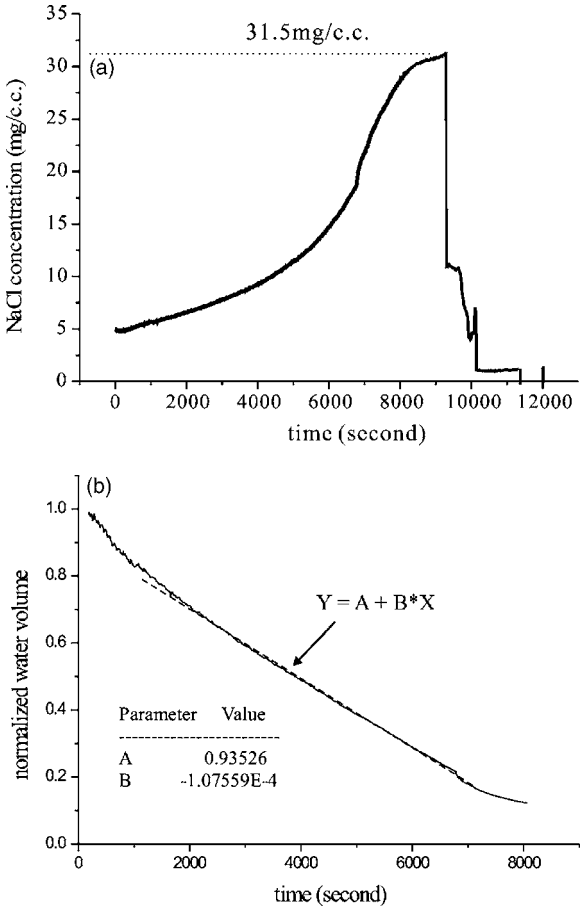

Fig. 5 (a) Measured salt concentration versus time. The initial volume of the salt solution was 30 μl and its concentration was 5% mg/cm^3. After ~150 min, the salt concentration reached saturation at ~31.5 mg/cm^3. (b) Volume of water versus time. The slope of the plot yields the evaporation rate of water. Initially, water has a large evaporation rate, which becomes ~0.2 μl/min for a long period (~100 min). The rate is calculated by linear fit to slope of the volume of water. The dashed line shows the fitting result.

concentration. The optical intensity increased with the concentration of salt. The measurements were made many times, yielding similar results. Notably, the optical detection limit of the PMT is $\sim 10^{-15}$ W, which is markedly below the measured intensity, which was in the order of nanowatts. However, Fig. 4(a) has ~0.3% fluctuations in the intensity measurement. The fluctuations were due to the limit of power stability of the laser.

The refractive indices of solutions with various salt concentrations were measured using a refractometer to determine the RIU sensitivities of the nanofiber probe sensor. Figure 4(b) plots the optical intensity versus the refractive index. The experiments confirm that the transmission increases with the refractive index of the surrounding medium. The error bars indicate the standard deviations over five measurements. The maximum deviation in the measured intensity is 2%. Note that the experimental results exhibit much better sensitivity than the FDTD predictions. The optical intensity was approximately tripled as the outside refractive index changed from 1.33 to 1.375. The experimental results show an RIU sensitivity of 4444 (% RIU^{-1}), suggesting an RIU resolution of 2.25×10^{-5} for the measurement of intensity at an optical power stability of 0.1%. This value is similar to that obtained using conventional prism-based system when the intensity changes near resonance are measured.[2] The gold coating may have contributed to the greater sensitivity. The sputtered coated gold film was not smooth. The SEM image reveals that the gold film comprised of nanometer islands. The nanometer surface roughness caused additional LSR at the fiber tip, and may have been responsible for the increase in sensitivity. Notably, the change in the intensity with the refractive index was fitted by a polynomial curve rather than a line. The intensity change is much larger than the FDTD predictions, so a nonlinear increase in the intensity of light is expected.

The nanotip fiber sensor has the advantages of good RIU sensitivity and a localized interaction region, enabling the dynamic properties of a very small volume of solution to be determined. For instance, a nanotip sensor can be used to determine the evaporation rate of a small drop of water on a glass slide. The evaporation rate importantly affects measurements of biologic samples on glass slides. The nanofiber sensor can be used to monitor the evaporation rate of water under different conditions if a relationship between the transmission intensity and concentration is established. In this paper, we

measured the transmission intensity versus salt concentration. This information can be used to determine the evaporation rate of water by recording the optical intensity changes. Figure 5(a) plots the measured concentration against time. The initial volume of salt solution was 30 μl and its concentration was 5% mg/cm^3. After it had remained under ambient conditions for 150 min, most of the water had evaporated and the NaCl solution was saturated ($\sim$31.5 mg/cm^3). Following saturation, no water was present in the tip. The tip was directly exposed to air and caused a drastic decrease in optical intensity. The simple relationship between the amount of water and the salt concentration, $V(0)C(0)=V(t)C(t)$, where $V(t)$ is the volume of water and $C(t)$ is the salt concentration, was used to calculate the evaporation rate of water. Figure 5(b) shows the volume of water against time. The slope of the plot is the evaporation rate of water under ambient conditions. Initially, the evaporating rate of water is high, $\sim$0.36 μl/min. Then, the volume of water is linearly decreased. The correlation coefficient, R for the linear fit is -0.99. The evaporation rate is 0.2 μl/min during a long period ($\sim$100 min).

In summary, a novel fiber optic biosensor based on the generation of SPWs near a nanotip is proposed. The nanofiber tip was coated with a thin film of gold. SPWs can couple to a gold surface and propagate to the end of the tip. Because most light in the tip is cut off, the nano-SPW sensor has a weak background. The nanofiber sensor reaches an RIU resolution of $\sim 2\times 10^{-5}$ at an optical power stability of 0.1%. Moreover, effective coupling of SPW occurs near the fiber tip. It requires only a very small sample volume. Unlike the conventional ATR approach, the nanofiber SPW sensor is simple and easy to use. It can be used to perform multiple detections using arrays of probes.

Acknowledgments

The authors would like to thank the National Science Council of the Republic of China, Taiwan (Contract No. NSC 93-2215-E-001-001) and the Nano Program of Academia Sinica, Taiwan, for financially supporting this research.

References

1. W. Knoll, "Interfaces and thin films as seen by bound welectromagnetic waves," *Annu. Rev. Phys. Chem.* **49**, 569–639 (1998).
2. J. Homola, S. S. Yee, and G. Gauglitz, "Surface plasmon resonance sensors: review," *Sens. Actuators B* **54**, 3–15 (1999).
3. C. Bariain, I. R. Matiasa, I. Romeo, J. Garrido, and M. Laguna, "Detection of volatile organic compound vapors by using a vapochromic material on a tapered optical fiber," *Appl. Phys. Lett.* **77**, 2274–2276 (2000).
4. R. Slavı'k, J. Homola, and J. Ctyroky, "Single-mode optical fiber surface plasmon resonance sensor," *Sens. Actuators B* **54**, 74–79 (1999).
5. A. Diez, M. V. Andres, and J. L. Cruz, "In-line fiber-optic sensors based on the excitation of surface plasma modes in metal-coated tapered fibers," *Sens. Actuators B* **73**, 95–99 (2001).
6. K. Mitsui, Y. Handa, and K. Kajikawa, "Optical fiber affinity biosensor based on localized surface plasmon resonance," *Appl. Phys. Lett.* **85**, 4231–4233 (2004).
7. S. Underwood and P. Mulvaney, "Effect of the solution refractive index on the color of gold colloids," *Langmuir* **10**, 3427–3430 (1994).
8. L. A. Lyon, M. D. Musick, P. C. Smith, B. D. Reiss, D. J. Pena, and M. J. Natan, "Surface plasmon resonance of colloidal Au-modified gold films," *Sens. Actuators B* **54**, 118–124 (1999).
9. M. A. Paesler and P. Moyer, *Near-Field Optics: Theory, Instrumentation, and Applications*, Wiley, New York (1996).
10. Taflove and S. C. Hagness, *Computational Electrodynamics: The Finite-Difference Time-Domain Method*, 2nd ed., Artech House, Boston (2000).
11. P. K. Wei, Y. C. Chen, and H. L. Kuo, "Systematic variation of polymer jacket fibers and the effects on tip etching dynamics," *J. Microsc.* **210**(3), 334–337 (2003).